RIMS Kôkyûroku Bessatsu
B61 (2017), 23–56

An invitation to Sato's postulates in micro-analytic S-matrix theory

By

Naofumi HONDA* and Takahiro KAWAI**

Acknowledgment We dedicate this paper to Professor H. Komatsu, who has organized the Japanese group in algebraic analysis by his enthusiastic activities to lead young students to the theory of hyperfunctions by giving a series of lectures in the University of Tokyo (1967∼1968) and organizing the Sato-Komatsu seminar (1968∼1970) and by trying with success to call the attention of Professor M. Sato to the application of the theory of hyperfunctions. We are most obliged to Professor Komatsu for all his trials, which are not only remarkable but also exceptional in the history of mathematics. ([K])

Abstract

By studying some basic examples in micro-analytic S-matrix theory we show how the trials toward the better understanding of Sato's postulates on the S-matrix lead us to find novel and intriguing problems in microlocal analysis. For the convenience of a microlocal analyst who has become interested in Sato's postulates we have included in Section 2 an illustrative example which shows how to use Landau-Nakanishi diagrams to detect singular points such as cusps in the Landau-Nakanishi surface.

§ 0. Introduction

The purpose of this article is to try to elucidate Sato's postulates on the S-matrix ([S]) by the detailed study of concrete examples. The renaissance of the interest of mathematical physicists in the resurgent theory enhances the value of studying the detailed analysis of Feynman integrals, which appear as the coefficients of perturbation series of the S-matrix in the power of the coupling constant, and at the same time

Received May 11, 2016. Revised September 12, 2016. Accepted September 12, 2016.
2010 Mathematics Subject Classification(s): Primary 81Q30; Secondary 32S40.
Key Words: *S-matrix, Feynman and phase space integrals, Sato's postulates, microlocal analysis.*
*Department of Mathematics, Faculty of Science, Hokkaido University, Sapporo, 060-0810 Japan.
Supported in part by JSPS KAKENHI Grant Number 15K04887.
e-mail: honda@math.sci.hokudai.ac.jp
**Research Institute for Mathematical Sciences, Kyoto University, Kyoto, 606-8502 Japan.
Supported in part by JSPS KAKENHI Grant Number 24340026.

we try in this paper to call the attention of young specialists in microlocal analysis to the pregnant and suggestive paper [S] of Sato. (We are most grateful to Professor O. Costin and Professor D. Sauzin who have kindly called our attention to the conference "Resurgence and Transseries in Quantum, Gauge and String Theories" held in 2014 at CERN as an evidence of the "renaissance of the interests in resurgent functions of physicists.") The plan of this paper is as follows:

In Section 1, we recall some basic notions and notations we use in this paper.

In Section 2, by using the simplest example of the sort, i.e., a triangle Feynman graph, we concretely show how to use the Landau-Nakanishi (=LN) diagram to find the concrete shape of the LN surface. Although the discussion in this section is an elementary one we believe that it will convince the reader of the nice chemistry between the LN diagram and microlocal analysis.

In Section 3, we recall Sato's postulates focusing on the points to be polished up in this paper and in our future studies. Together with them we briefly describe some of our previous results which are immediately related to Sato's postulates.

In Section 4, we show how a complemented graph ([HK3]) can be effectively used in analyzing phase space integrals associated with non-external graph such as T_3 (cf. [HKS]). Here a non-external graph means a Feynman graph which contains a non-external vertex, that is, a vertex upon which no external line is incident, and a complemented graph $\tilde{G}$ of a non-external graph G is, by definition, the graph obtained by the addition of an external line to each non-external vertex of G. We hope that introducing complemented graphs into our study fits in with Sato's philosophy to the effect that the dynamical completeness should be attained through the analysis of non-observable quantities. ([S, p.15])

In Section 5, we list up several problems which we hope to be useful for further developing the research in micro-analytic S-matrix theory and related problems in microlocal analysis. At the end of this section we briefly describe what are bubble diagram functions and how they are related to the results in this paper.

§ 1. Preliminaries

In order to make this paper a self-contained one for specialists in microlocal analysis, we recall the definition of Feynman graph G, Feynman integral F_G and phase space integral I_G associated with G, and the Landau-Nakanishi equations determined by G. In what follows we normally abbreviate "Landau-Nakanishi" to LN, like LN equations, LN diagrams, LN surfaces, LN varieties, etc.

Definition 1.1. (i) A Feynman graph G is a graph consisting of

(1.1) finitely many points $V_1, V_2, \cdots, V_{n'}$, which are called vertices, (1.2) finitely many line segments, $L_1, L_2, \cdots, L_N$, which are called internal lines,

and

(1.3) finitely many half-lines $L_1^e, L_2^e, \cdots, L_n^e$, which are called external lines,

which satisfy the following conditions (1.4), (1.5) and (1.6):

(1.4) each end point W_l^+ and W_l^- of L_l $(l = 1, 2, \cdots, N)$ coincides with some of V_j $(j = 1, \cdots, n')$,

$$W_l^+ \neq W_l^- \quad (l = 1, 2, \cdots, N), \tag{1.5}$$

(1.6) the (unique) end point of L_r^e $(r = 1, 2, \cdots, n)$ coincides with some of V_j $(j = 1, \cdots, n')$.

We further assume

(1.7) a ν-dimensional vector $p_r = (p_{r,0}, p_{r,1}, \cdots, p_{r,\nu-1})$ is attached to each external line L_r^e,

(1.8) a strictly positive constant m_l is attached to each internal line L_l,

and

(1.9) each internal line and each external line is oriented, and the orientation is designated by an arrow like $\rightarrow\!\!-$. (To simplify the figures we often omit the arrow.)

(ii) The incidence number $[j : l]$ for a pair of a vertex V_j and an internal line L_l is given by the following:

$$[j : l] = \begin{cases} +1 & \text{when } L_l \text{ ends at } V_j \\ -1 & \text{when } L_l \text{ starts from } V_j \\ 0 & \text{otherwise.} \end{cases} \tag{1.10}$$

The incidence number $[j : r]$ for a pair of a vertex V_j and an external line L_r^e is defined in the same manner.

(iii) It follows from (1.4) and (1.5) that, for each internal line L_l there uniquely exists a vertex V_{j_0} such that $[j_0 : l] = +1$, and such j_0 shall be denoted by $j^+(l)$. Similarly we define $j^-(l)$ and $j(r)$.

Example 1.1. Triangle Feynman graph T_1 is given by the following:

(1.11)

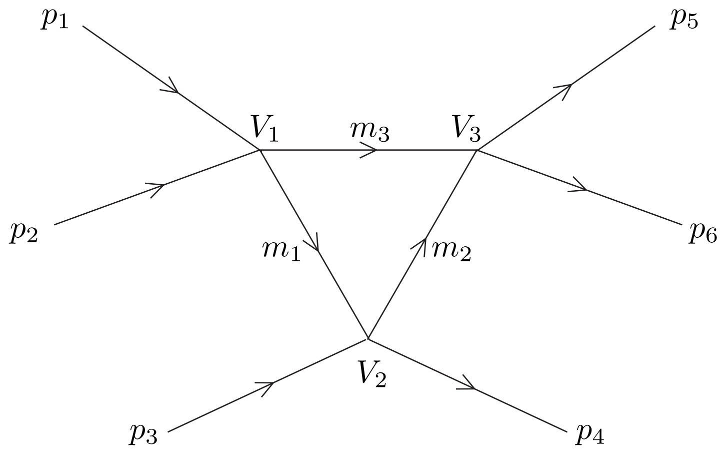

Definition 1.2. (i) The Feynman integral $F_G(p)$ associated with a Feynman graph G is formally (i.e., being set aside its well-definedness as a hyperfunction) given by the following:

$$F_G(p) = F_G(p_1, p_2, \cdots, p_n) \tag{1.12}$$
$$= \int \cdots \int \frac{\prod_{j=1}^{n'} \delta^\nu\Big(\sum_{r=1}^{n}[j:r]p_r + \sum_{l=1}^{N}[j:l]k_l\Big)}{\prod_{l=1}^{N}\left(k_l^2 - m_l^2 + i0\right)} \prod_{l=1}^{N} d^\nu k_l.$$

Here, and in what follows, δ^ν stands for the ν-dimensional δ-function, and, for a ν-dimensional vector $k = (k_0, k_1, \cdots, k_{\nu-1})$ its square k^2 always means

$$k^2 = k_0^2 - \sum_{\mu=1}^{\nu-1} k_\mu^2. \tag{1.13}$$

(ii) The Feynman amplitude $f_G(p)$ associated with a Feynman graph G is the function obtained by factorizing out the over-all conservation δ-function $\delta^\nu\big(\sum_{j,r}[j:r]p_r\big)$ from $F_G(p)$; that is,

$$F_G(p) = \delta^\nu\big(\sum_{j,r}[j:r]p_r\big) f_G(p). \tag{1.14}$$

(iii) The phase space integral $I_G(p)$ associated with a Feynman graph G is formally given by the following:

$$I_G(p) = \int \cdots \int \prod_{j=1}^{n'} \delta^\nu\Big(\sum_{r=1}^{n}[j:r]p_r + \sum_{l=1}^{N}[j:l]k_l\Big) \prod_{l=1}^{N} \delta^+\big(k_l^2 - m_l^2\big) \prod_{l=1}^{N} d^\nu k_l, \tag{1.15}$$

where $\delta^+(k_l^2 - m_l^2)$ stands for $\delta(k_l^2 - m_l^2)$ multiplied by the Heaviside function $Y(k_{l,0})$ of the 0-th component of k_l, i.e.,

$$\delta(k_l^2 - m_l^2)Y(k_{l,0}). \tag{1.16}$$

We also denote by $I_G(p)$ the function obtained by factorizing out the over-all δ-function $\delta^\nu(\sum_{j,r}[j:r]p_r)$ from $I_G(p)$, if there is no fear of confusion.

Remark 1.1. In what follows, we use the definition (1.13) of k^2 to identify $\mathrm{grad}_k k^2$ with k; for example, the vector k_l in the right-hand side of (1.19) below is $\mathrm{grad}_{k_l} k_l^2$ if we think over its origin.

Definition 1.3. (i) Landau-Nakanishi (=LN) equations for $(p;u) = (p_1, \cdots, p_n; u_1, \cdots, u_n)$ $(\in \mathbb{R}^{2\nu n})$ determined by a Feynman graph G are given by the following set of equations (1.17)∼(1.20), where k_l $(l = 1, 2, \cdots, N)$, V_j $(j = 1, 2, \cdots, n')$ and a are in $\mathbb{R}^\nu$ and α_l $(l = 1, 2, \cdots, N)$ is a real number (called a LN constant) with $\sum_{l=1}^{N}|\alpha_l| > 0$:

$$\sum_{r=1}^{n}[j:r]p_r + \sum_{l=1}^{N}[j:l]k_l = 0 \quad \text{for } j = 1, 2, \cdots, n', \tag{1.17}$$

$$\alpha_l(k_l^2 - m_l^2) = 0 \quad \text{with} \quad k_{l,0} > 0 \quad \text{for } l = 1, 2, \cdots, N, \tag{1.18}$$

$$V_{j^+(l)} - V_{j^-(l)} = \alpha_l k_l \quad \text{for } l = 1, 2, \cdots, N, \tag{1.19}$$

$$u_r = [j(r):r](V_{j(r)} + a) \quad \text{for } r = 1, 2, \cdots, n. \tag{1.20}$$

(ii) Landau-Nakanishi (=LN) diagram is, by definition, a Feynman graph whose internal line L_l is equipped with $(\alpha_l, k_l)(\in \mathbb{R}^{1+\nu})$

Example 1.2. Triangle LN diagram T_1 is given by the following:

(1.21)

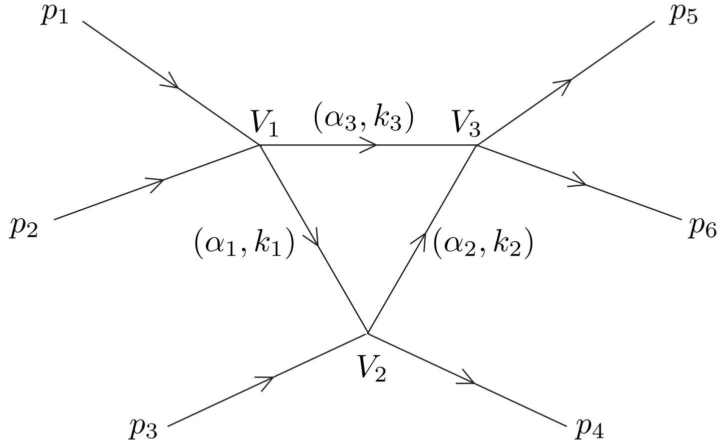

Here, and in what follows, we omit m_l attached to L_l in a Feynman graph, as we assume in this paper that all m_l's are supposed to be equal to 1 unless otherwise stated. (However we sometimes use the redundant expression such as " $m_l^2 = 1$" to emphasize that the number 1 is actually a special value of m_l^2.) In this paper we usually omit α_l for the technical simplicity in preparing figures which are needed in our reasoning.

Remark 1.2. The existence of a free vector a in (1.20) implies that an LN diagram may be translated arbitrarily as a whole in $\mathbb{R}^\nu$. As a specialist in microlocal analysis will imagine, this fact is a counterpart of the fact that $F_G(p)$ contains the over-all conservation δ-function as its factor, i.e., $F_G(p) = \delta^\nu\big(\sum_{j,r}[j : r]p_r\big) f_G(p)$. In view of these facts we normally consider the problem on $\mathbb{R}^{\nu(n-1)} = \big\{p \in \mathbb{R}^{\nu n}; \sum_{j,r}[j : r]p_r = 0\big\}$ or $T^*\mathbb{R}^{\nu(n-1)}$ without so mentioning explicitly.

Remark 1.3. The vector k_l attached to the internal line L_l in an LN diagram has a dual meaning; k_l in (1.19) is $\mathrm{grad}_{k_l} k_l^2$, which is a dual (with respect to the Minkowski metric) vector of k_l in (1.17) and (1.18). Hence LN equations define a subvariety $\mathscr{L}(G)$ of $T^*\mathbb{R}_p^{\nu n}$ which is conical, that is, homogeneous with respect to the cotangential component u. We call the variety as the LN variety associated with G, and we call its projection to the base manifold $\mathbb{R}^{\nu n}$ as the LN surface with some slight abuse of the language. (We note that some component of an LN "surface" is actually of higher codimension as is pointed out in [HK1].) In what follows we let $L(G)$ denote the LN surface associated with G. We introduce the subsets of $\mathscr{L}(G)$ and $L(G)$ by Definition 1.4 below, where π denotes the canonical projection from $T^*\mathbb{R}_p^{\nu n}$ or $T^*\mathbb{R}_p^{\nu(n-1)}$ to $\mathbb{R}_p^{\nu n}$ or $\mathbb{R}_p^{\nu(n-1)}$.

Definition 1.4. (i) The leading part $\mathscr{L}^\times(G)$ of $\mathscr{L}(G)$ is, by definition, the totality of solutions $(p; u)$ of LN equations with $\alpha_l \neq 0$ $(l = 1, \cdots, N)$.

(ii) The positive-α part $\mathscr{L}^+(G)$ of $\mathscr{L}(G)$ is, by definition, the totality of solutions $(p; u)$ of LN equations with $\alpha_l \geq 0$ $(l = 1, \cdots, N)$ (and $\alpha_{l_0} > 0$ for some l_0).

(iii) The leading positive-α part $\mathscr{L}^\oplus(G)$ of $\mathscr{L}(G)$ is, by definition, the totality of solutions of $(p; u)$ of LN equations with $\alpha_l > 0$ $(l = 1, \cdots, N)$.

(iv) The leading part $L^\times(G)$, the positive-α part $L^+(G)$ and the leading positive-α part $L^\oplus(G)$ of $L(G)$ are respectively defined by $\pi(\mathscr{L}^\times(G))$, $\pi(\mathscr{L}^+(G))$ and $\pi(\mathscr{L}^\oplus(G))$.

Remark 1.4. In what follows we often use the abbreviated wording "a leading positive-α LN surface" etc. instead of "the leading positive-α part of a LN surface" etc.

Remark 1.5. The relevance of LN equations to the cotangent bundle was first recognized by H. P. Stapp and his collaborators ([CS], [IS]) through the Fourier transformation of the macroscopic causality condition.

Remark 1.6. In this paper we restrict our consideration to the case where $\nu = 2$ unless otherwise stated, so that we may make full use of figures prepared with the help of a computer. We believe the core part of our reasoning below should be also validated when $\nu = 4$, although we have not yet tried seriously to think over this point. In what follows we also assume that all m_l's are equal to the same positive number m (in most cases 1). Concerning this restriction we imagine that it would be an interesting problem to study the situation where m_l's are not necessarily mutually equal, or rather the situation where m_l's are regarded as independent variables.

§ 2. An example of how-tos for locating singular points of a Landau-Nakanishi surface with the help of the relevant Landau-Nakanishi diagram

In this section we concretely show how an LN diagram is effectively used in finding singular points of an LN surface. Although computer-assisted study is much more powerful and far-reaching (e.g. [HK2]), we hope the reasoning in this section will be helpful for a specialist in microlocal analysis (hereafter abbreviated as a microlocal analyst) to become familiar with LN diagrams and LN surfaces, which are essential languages in explaining Sato's postulates.

In what follows we consider the following simplest example of the sort: we consider the LN surface associated with triangle LN diagram T_1 given in Example 1.2. In order to simplify the figures and explanations in our discussion below we introduce following notations:

$$A = V_1, \quad B = V_2, \quad C = V_3, \tag{2.1}$$

$$p_A = p_1 + p_2, \quad p_B = p_4 - p_3, \quad p_C = p_5 + p_6, \tag{2.2}$$

$$u_A = -V_1 = -A, \quad u_B = V_2 = B, \quad u_C = V_3 = C. \tag{2.3}$$

As the over-all energy-momentum conservation entails that p_B is equal to $p_A - p_C$, the LN surface $L(T_1)$ is described in $\mathbb{R}^4_{(p_A, p_C)}$.

Our main concern in this section is $[L^\times(T_1)]$, the (topological) closure of $L^\times(T_1)$, and hence we may assume

$$k_l^2 = m_l^2 = 1, \quad k_{l,0} > 0 \quad (l = 1, 2, 3) \tag{2.4}$$

in what follows. Then by using an appropriate Lorentz transformation we may assume without loss of generality the following:

$$p_A = (x, x), \quad p_C = (y, z) \tag{2.5}$$

(2.6) $$k_3 = (s, s^{-1}),\ k_1 = (s^{-1}, s),\ k_2 = (t, t^{-1}) \quad (s, t > 0).$$

In particular, we have

(2.7) $$x = s + s^{-1},\ y = s + t,\ z = s^{-1} + t^{-1}.$$

Here we emphasize that the assumption $\nu = 2$ is essential in giving the parametrization (2.6), which is substantially useful in our computer-assisted works ([HK1], [HK2]). In order to simplify the figures we label k_1, k_2 and k_3 respectively by s^{-1}, t, s (i.e., the first component in the parametrization (2.6)). Thus the LN diagram is labelled as follows:

(2.8)

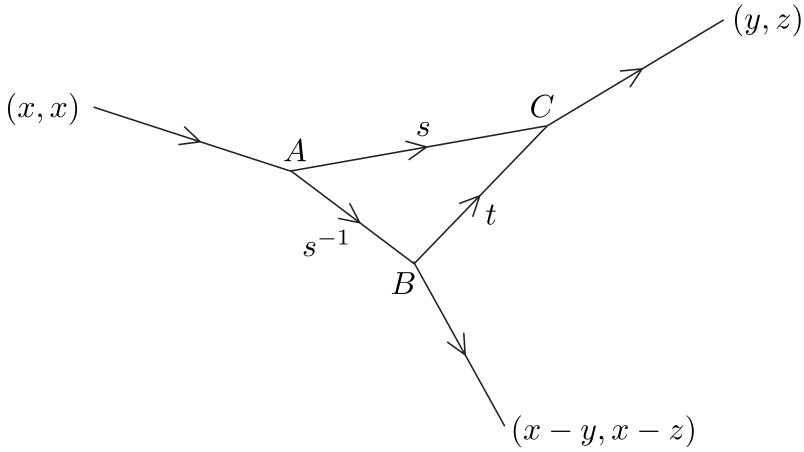

We now change (s, t) and trace the point (p_A, p_C) determined by the LN diagram by (2.8), and in our discussion we use the following reduced symbol as a simplified form of (2.8):

(2.9)

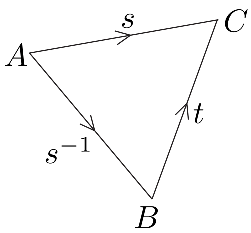

that is, we often omit the external lines if there is no fear of confusions. Here we call the attention of the reader to the relation (2.7). We also note that, when we use the reduced symbol (2.9), we normally let α_{AB}, α_{BC} and α_{AC} respectively denote the LN constant attached to internal lines L_1, L_2 and L_3. In accordance with this notation, we use k_{AB}, k_{BC} and k_{AC} to denote k_1, k_2 and k_3 respectively.

As a microlocal analyst readily finds, $[L^{\times}(T_1)]$ describes the location of singular points of I_{T_1}, the phase space integral associated with T_1, and, with the notations given by (2.2) and (2.3), the u-vector (u_A, u_B, u_C) describes the cotangential component of S.S.$I_{T_1}(p)$, the singularity spectrum of $I_{T_1}(p_A, p_B, p_C)$. It will be also easy for a microlocal analyst to observe the following:

(2.10) $L^+(T_1)$ describes the location of singular points of f_{T_1}, the Feynman amplitude associated with T_1;

(2.11) in particular, f_{T_1} may be singular on the LN surface associated with the so-called contracted diagram of T_1, that is, the diagram with some LN constant being 0 like 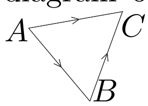

with $\alpha_{BC} = 0$.

In order to visualize (2.10) and (2.11) rather symbolically, physicists normally use the following figure:

(2.12)

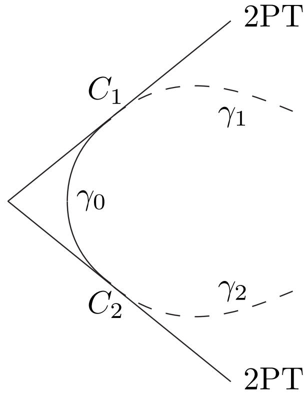

Among several (possibly symbolic) messages we find in figure (2.12), we emphasize the following:

(2.13) $L^\oplus(T_1)$ is given by a smooth surface γ_0;

(2.14) At C_1 (resp., C_2) in $[\gamma_0]$, the closure of γ_0, LN constant α_{BC} (resp., α_{AB}) vanishes;

(2.15) $[\gamma_0] \cup \gamma_1$ (resp., $[\gamma_0] \cup \gamma_2$) is a smooth surface near C_1 (resp., C_2) and touches with 2PT (=2 particle threshold) given by $L^\oplus$ 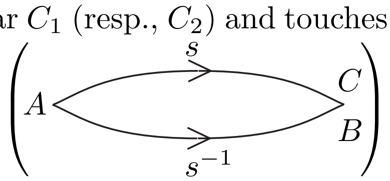

(resp., $L^\oplus$ 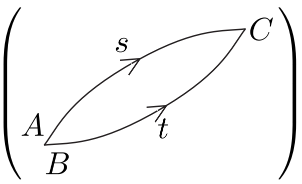

) at C_1 (resp., C_2);

(2.16) LN constant α_{BC} (resp., α_{AB}) is negative in γ_1 near C_1 (resp., in γ_2 near C_2) and f_{T_1} is not singular there, (2.17) Although γ_1 and γ_2 are drawn by dotted lines in conjunction with the non-singular property of f_{T_1} there, I_{T_1} may be singular on γ_1 and γ_2; the singularities originate from some of $(k_l^2 - m_l^2 - i0)^{-1}Y(k_{l,0})$ $(l = 1, 2, 3)$ contained in $\delta^+(k_l^2 - m_l^2)$ in the integrand of I_{T_1}.

Now having in mind these messages from (2.12), a symbolic figure of a 2-dimensional slice of $L^+(T_1)$, we raise the following questions:

(2.18) Is there any interaction of γ_1 and γ_2 if we consider the problem in the 3-dimensional space $\mathbb{R}^3_{(x,y,z)}$?

(2.19) Are there any singular points in $[L^\times(T_1)]$ outside γ_0?

In what follows we answer these questions by "playing with LN diagram 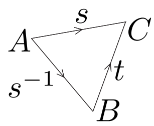

.

We begin our discussion by noting the following fact, which can be readily confirmed:

(2.20) γ_0 consists of two parts $\gamma_0^{1<}$ and $\gamma_0^{<1}$,

where

(2.21) $\gamma_0^{1<}$ consists of points in $L^\oplus(T_1)$ with $1 < s < t$,

and

(2.22) $\gamma_0^{<1}$ consists of points in $L^\oplus(T_1)$ with $t < s < 1$.

We note that (2.7) entails

(2.23) $y > z$ on $\gamma_0^{1<}$,

and

(2.24) $y < z$ on $\gamma_0^{<1}$.

Let us begin our journey in $[L^\times(T_1)]$ starting from a point $\sigma_{0,+}$ in $\gamma_0^{1<}$ which is determined by the following LN diagram $\Sigma_{0,+}$:

(2.25) $\Sigma_{0,+}$: 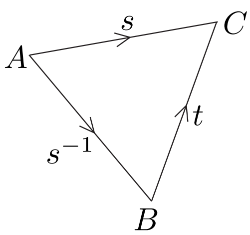

with $1 < s < t$.

We first decrease s to reach 1 so that we encounter C_1, where $[\gamma_0]$ touches with $\{p_A^2 = 4\}$; the LN diagram corresponding to C_1 is

(2.26)

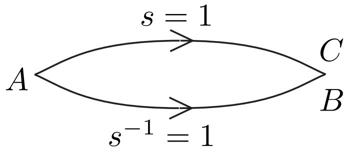

with $\alpha_{BC} = 0$.

In order to continue our journey to γ_1 we further decrease s to find the following LN diagram C_1^+:

(2.27) C_1^+ :

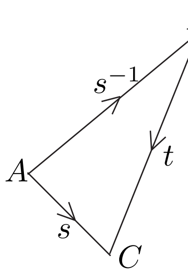

with $s < 1 < s^{-1} < t$,

where

$$\alpha_{AB},\ \alpha_{AC} > 0,\ \alpha_{BC} < 0. \tag{2.28}$$

Here, to realize the LN diagram we have to assume (2.28) as the relative location of B and C in (2.27) is different from that in (2.25). As a microlocal analyst readily sees, the relation (2.28) indicates that the singularity of I_{T_1} there comes from $(k_{BC}^2 - 1 - i0)^{-1}Y(k_{BC,0})$ in $\delta^+(k_{BC}^2 - 1)$ in the integrand of I_{T_1}.

We next fix s (< 1) and let t decrease in (2.27) to realize the following diagram D_1:

(2.29) D_1 :

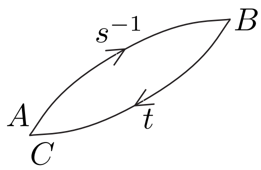

with

$$t = s^{-1} > 1, \tag{2.30}$$

$$\alpha_{AB} > 0,\ \alpha_{AC} = 0,\ \alpha_{BC} < 0. \tag{2.31}$$

We also denote by D_1^- (resp., D_1^+) the configuration which we encounter just before (resp., after) finding D_1, that is,

(2.32) D_1^- :

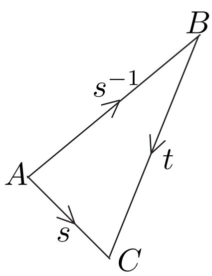

with

$$1 < s^{-1} < t, \tag{2.33}$$

$$\alpha_{AB} > 0,\ \alpha_{AC} > 0,\ \alpha_{BC} < 0, \tag{2.34}$$

and

(2.35) D_1^+ :

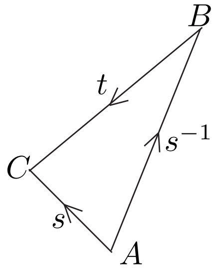

with

$$1 < t < s^{-1}, \tag{2.36}$$

$$\alpha_{AB} > 0,\ \alpha_{AC} < 0,\ \alpha_{BC} < 0. \tag{2.37}$$

Although the diagrammatic structure of D_1 and those of $D_1^{\pm}$ might look quite different, the associated LN geometry smoothly changes. Since this fact is a starting point of our study below, we summarize the situation as follows:

Lemma 2.1. *Let* $\mathscr{L}^{\times}(T_1)|_{\Omega_1^+(\varepsilon)}$ $(0 < \varepsilon \ll 1)$ *denote the set of solutions* (p, u) *associated with* T_1 *and which satisfy the following conditions:*

$$\alpha_{AB} > 0,\ \alpha_{BC} < 0,\ \alpha_{AC} \neq 0, \tag{2.38}$$

$$|st - 1| < \varepsilon, \tag{2.39}$$

$$0 < s < 1. \tag{2.40}$$

Then its closure $[\mathscr{L}^{\times}(T_1)|_{\Omega_1^+(\varepsilon)}]$ *is smooth. Furthermore its projection to the base manifold* $\mathbb{R}^3_{(x,y,z)}$ *is also non-singular.*

Proof. Let (P_0, U_0) denote the solution of LN configuration D_1. Then it follows from (2.7) and (2.30) that

$$x = y = z \gneqq 2 \tag{2.41}$$

holds at P_0. Hence

$$s = s_-(x) \underset{\text{def}}{=} \left(x - \sqrt{x^2-4}\right)/2 \tag{2.42}$$

is biholomorphic between s and x. We note that $s_-(x)$ is a solution of

$$s^2 - xs + 1 = 0, \tag{2.43}$$

which is smaller than 1 near P_0. Then it is clear that

$$\varphi_1(x,y,z) = z - \left(s_-(x)^{-1} + (y - s_-(x))^{-1}\right) \tag{2.44}$$

is holomorphic near P_0 with $\operatorname{grad}_{(x,y,z)}\varphi_1$ being different from 0. Since the projection of $[\mathscr{L}^\times(T_1)|_{\Omega_1^+(\varepsilon)}]$ is given by $\{\varphi_1 = 0\}$ for sufficiently small ε, the non-singularity of this set is clear. To confirm the non-singularity of $[\mathscr{L}^\times(T_1)|_{\Omega_1^+(\varepsilon)}]$ we construct holomorphic functions $\alpha_{AC}(s,t)$ and $\alpha_{BC}(s,t)$ for (s,t) satisfying (2.39) and (2.40) so that the following closed loop condition may be satisfied:

$$\alpha_{AC}\begin{pmatrix} s \\ s^{-1}\end{pmatrix} = \alpha_{AB}\begin{pmatrix} s^{-1} \\ s\end{pmatrix} + \alpha_{BC}\begin{pmatrix} t \\ t^{-1}\end{pmatrix} \tag{2.45}$$

with the normalization

$$\alpha_{AB} = 1. \tag{2.46}$$

One can then easily find

$$\alpha_{AC} = \frac{t^2s^2-1}{t^2-s^2}\ , \tag{2.47}$$

$$\alpha_{BC} = \frac{ts^{-1}(s^4-1)}{t^2-s^2}. \tag{2.48}$$

Using these results we find

$$u_B = \begin{pmatrix} s^{-1} \\ s\end{pmatrix}, \tag{2.49}$$

$$u_C = \left(\frac{t^2s^2-1}{t^2-s^2}\right)\begin{pmatrix} s \\ s^{-1}\end{pmatrix} \tag{2.50}$$

by setting $u_A = 0$, which realize configuration D_1 and $D_1^\pm$, together with (2.7). Thus we find $[\mathscr{L}^\times(T_1)|_{\Omega_1^+(\varepsilon)}]$ is non-singular. This completes the proof of the lemma.

We now try to find the counterpart of the above journey when we start from a point $\sigma_{0,-}$ in $\gamma_0^{<1}$, that is, when we start from a point where the following configuration is realized:

(2.51) $\Sigma_{0,-}$:
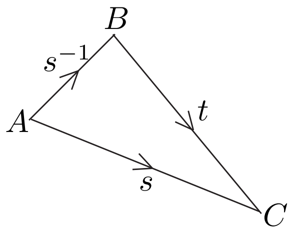

with $t < s < 1$.

Here we choose s close to the value of s in (2.27) to fix the situation. This time we let t increase to attain

(2.52)
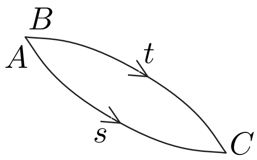

with

$$t = s < 1, \tag{2.53}$$

$$\alpha_{AB} = 0. \tag{2.54}$$

Then we encounter C_2, where $[\gamma_0]$ touches with $\{p_C^2 = 4\}$. After reaching C_2 we continue our journey to enter γ_2 by letting t increase, and we find

(2.55) C_2^+ :
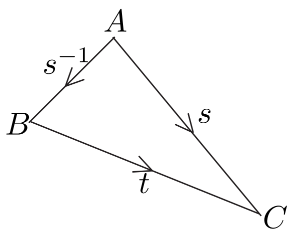

, $s < t$.

with

$$\alpha_{AB} < 0, \ \alpha_{AC}, \alpha_{BC} > 0. \tag{2.56}$$

By keeping s intact, we further increase t in (2.55) to realize the following diagram D_2:

(2.57) D_2 :
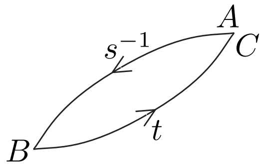

with

$$1 < s^{-1} = t, \tag{2.58}$$

(2.59) $$\alpha_{AB} < 0,\ \alpha_{AC} = 0,\ \alpha_{BC} > 0.$$

Just after (resp., before) meeting the point determined by D_2, we find D_2^+ (resp., D_2^-) given below:

(2.60) D_2^+ :

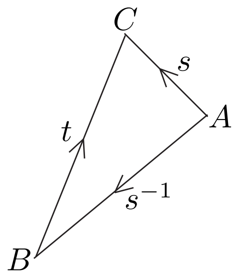

with

(2.61) $$1 < s^{-1} < t,$$

(2.62) $$\alpha_{AB}, \alpha_{AC} < 0,\ \alpha_{BC} > 0,$$

and

(2.63) D_2^- :

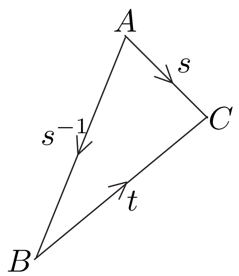

with

(2.64) $$1 < t < s^{-1},$$

(2.65) $$\alpha_{AB} < 0,\ \alpha_{AC}, \alpha_{BC} > 0.$$

As the constraint (2.61) is the same as (2.33), we may assume that D_1^- and D_2^+ are realized by the same set of parameters (s, t); actually it suffices to choose the value of s at the starting point $\sigma_{0,-}$ of the current journey to be the same as the value s in (2.27). We note that in the current journey we change only t, with s being fixed. Then it follows from (2.7) that the solution (p, u) of LN equations for D_1^- and that for D_2^+ share the same value p; in order to compare the u-component of the solution (p, u) of LN equation for D_1^- and that for D_2^+, let us present the following figure (2.66) combining figure (2.32) and figure (2.60): in figure (2.66) we set the vertex A at the origin both for D_1^- and D_2^+, and we let $(B(D_1^-), C(D_1^-))$ (resp., $(B(D_2^+), C(D_2^+)))$ denote the location of vertices (B, C) in D_1^- (resp., D_2^+).

(2.66)

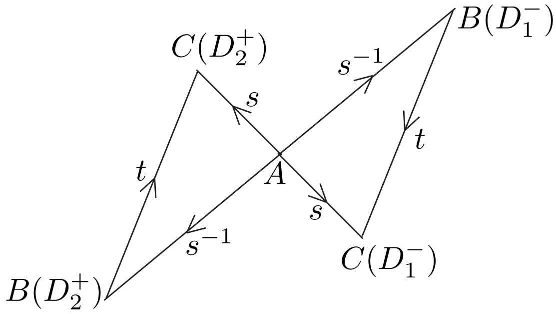

One immediately sees that $(B(D_1^-), C(D_1^-))$ and $(B(D_2^+), C(D_2^+))$ are located symmetrically with respect to the origin. Otherwise stated, the u-component for D_1^- and that for D_2^+ are of the opposite sign. The situation is exactly the same for the pair (D_1, D_2) and the pair (D_1^+, D_2^-), as the following figures indicate:

(2.67)

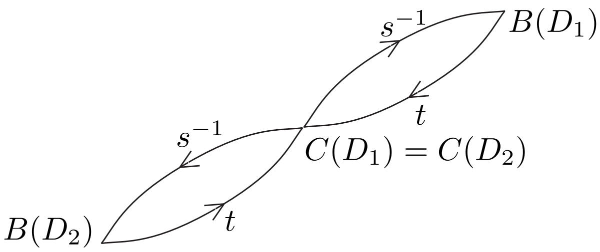

(Cf. (2.29) and (2.57)),

(2.68)

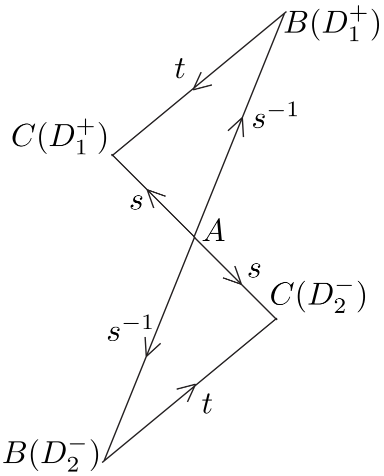

(Cf. (2.35) and (2.63)).

We have thus found two paths in $[L^\times(T_1)]$; one that starts from a point $\sigma_{0,+}$ in $\gamma_0^{1<}$ and ends at a point p_1 which is determined by LN diagram D_1^+ and lies in $\{\varphi_1(p) = 0\}$, and one that starts from a point $\sigma_{0,-}$ in $\gamma_0^{<1}$ and ends at the same point p_1 which is determined also by LN diagram D_2^-. An important observation is that the u-component of the solution of LN equations associated with D_1^+ is of the opposite sign of that associated with D_2^-. In order to visualize our argument we put the following rather symbolic labels to these paths. In what follows we call the path from $\sigma_{0,+}$ (resp., $\sigma_{0,-}$) as the route R_1 (resp., R_2).

$$R_1 : \Sigma_{0,+} \xrightarrow{s\downarrow} C_1^+ \xrightarrow{t\downarrow} D_1^- \xrightarrow{t\downarrow} D_1, \tag{2.69}$$

$$R_2 : \Sigma_{0,-} \xrightarrow{t\uparrow} C_2^+ \xrightarrow{t\uparrow} D_2 \xrightarrow{t\uparrow} D_2^+. \tag{2.70}$$

Here the mark "$s\downarrow$" etc. indicate that "we let s decrease" etc. For the convenience of the reader here we recall some characteristic features of LN diagrams in the above labelling:

(2.71) $1 < s < t \quad \text{in } \Sigma_{0,+}$,

(2.72) $s < 1 < s^{-1} < t \quad \text{in } C_1^+$,

(2.73) $1 < s^{-1} < t$ and $\alpha_{AB}, \alpha_{AC} > 0 \quad \text{in } D_1^-$,

(2.74) $1 < s^{-1} = t$, $\alpha_{AB} > 0$ and $\alpha_{AC} = 0 \quad \text{in } D_1$;

(2.75) in $\Sigma_{0,-}$ we assume $t < s < 1$ with s close to the value of s in (2.72),

(2.76) $s < t$ and $\alpha_{AB} < 0 \quad \text{in } C_2^+$,

(2.77) $1 < s^{-1} = t$ and $\alpha_{AB} < 0$ and $\alpha_{AC} = 0 \quad \text{in } D_2$,

(2.78) $1 < s^{-1} < t$ and $\alpha_{AB}, \alpha_{AC} < 0 \quad \text{in } D_2^+$.

Using a similar labelling, we now consider another pair of routes $\tilde{R}_1$ and $\tilde{R}_2$:

$$\tilde{R}_1 : \Sigma_{0,-} \xrightarrow{s\uparrow} \tilde{C}_1^+ \xrightarrow{t\uparrow} \tilde{D}_1^- \xrightarrow{t\uparrow} \tilde{D}_1 \xrightarrow{t\uparrow} \tilde{D}_1^+, \tag{2.79}$$

$$\tilde{R}_2 : \Sigma_{0,+} \xrightarrow{t\downarrow} \tilde{C}_2^+ \xrightarrow{t\downarrow} \tilde{D}_2^- \xrightarrow{t\downarrow} \tilde{D}_2 \xrightarrow{t\downarrow} \tilde{D}_2^+, \tag{2.80}$$

where

(2.81) $\tilde{C}_1^+$:

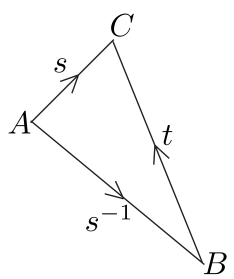

with $1 < s,\ \alpha_{BC} < 0$,

(2.82) $\tilde{D}_1^- :$ 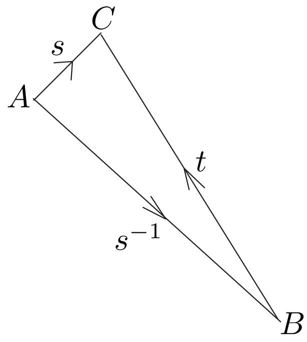

with $\alpha_{AC} > 0,\ \alpha_{BC} < 0,$

(2.83) $\tilde{D}_1 :$ 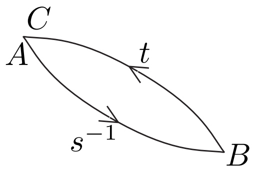

with $t = s^{-1} < 1,\ \alpha_{AC} = 0,$

(2.84) $\tilde{D}_1^+ :$ 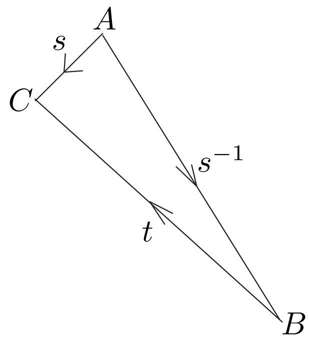

with $\alpha_{AC}, \alpha_{BC} < 0,$

(2.85) $\tilde{C}_2^+ :$ 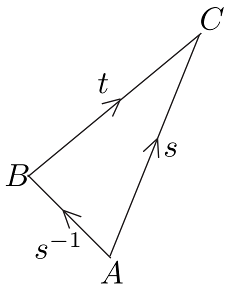

with $s^{-1} < t < s,\ \alpha_{AB} < 0,\ \alpha_{AC}, \alpha_{BC} > 0,$

(2.86) $\tilde{D}_2^- :$ 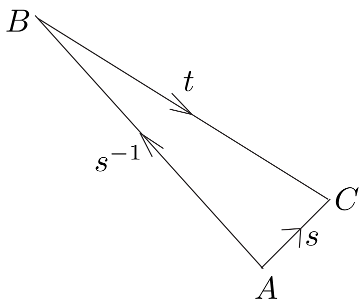

with $s^{-1} < t,\ \alpha_{AB} < 0,\ \alpha_{AC}, \alpha_{BC} > 0,$

(2.87) $\tilde{D}_2 :$ 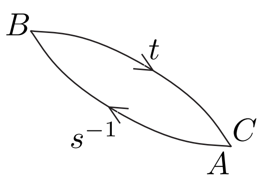

with $t = s^{-1} < 1,\ \alpha_{AB} < 0,\ \alpha_{AC} = 0,$

(2.88) $\tilde{D}_2^+$:

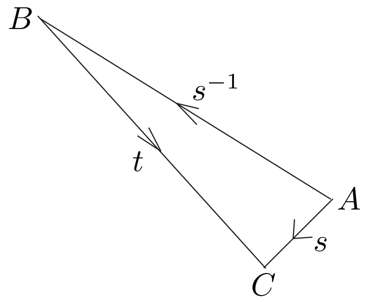

with $t < s^{-1} < 1,\ \alpha_{AB}, \alpha_{AC} < 0.$

The LN geometry determined by the triplet $(\tilde{D}_1, \tilde{D}_1^{\pm})$ (resp., $(\tilde{D}_2, \tilde{D}_2^{\pm})$) resembles to that determined by the triplet $(D_1, D_1^{\pm})$ (resp., $(D_2, D_2^{\pm})$); actually, if we define $\Omega_2^+(\varepsilon)$ by the conditions (2.89), (2.90) and (2.91) to be given below and use $\Omega_2^+(\varepsilon)$ as a substitute for $\Omega_1^+(\varepsilon)$ in Lemma 2.1, then we find that the projection of $[\mathscr{L}^\times(T_1)|_{\Omega_2^+(\varepsilon)}]$ to the base manifold defines a non-singular hypersurface $\{\varphi_2(p) = 0\}$ which passes P_0 for (s, t) $= (s, s^{-1})$:

(2.89) $$\alpha_{AB} > 0,$$

(2.90) $$|st - 1| < \varepsilon,$$

(2.91) $$1 < s.$$

Furthermore the location of the vertex B of D_1, D_2, $\tilde{D}_1$ and $\tilde{D}_2$ is as follows:

(2.92)

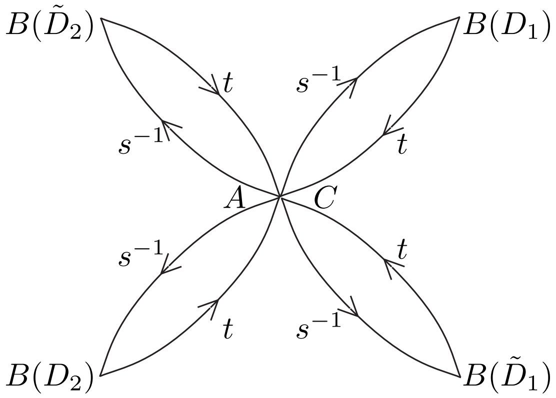

Here $B(D_1)$ etc. denote the location of the vertex B in D_1 etc., and $\alpha_{AB} > 0$ (resp., $\alpha_{AB} < 0$) for the labelling in the right (resp., left) half part of (2.92). This figure indicates

(2.93) $$\{\varphi_1 = 0\} \quad \text{and} \quad \{\varphi_2 = 0\}$$

intersect transversally along

(2.94) $$\Delta = \{(x, y, z) \in \mathbb{R}^3; x = y = z > 2\}.$$

Thus, by following up on the movement of LN diagrams, we have concretely confirmed that $[L^\times(T_1)]$ has self-intersection points along Δ. Our argument also shows that each point P_0 in Δ is relevant to both γ_1 and γ_2. Actually paths R_1 and $\tilde{R}_2$ both start from $\sigma_{0,+}$ and pass through a point P_0 in Δ; the former passes C_1, then moves in the region γ_1, satisfying

$$\alpha_{BC} < 0,\ \alpha_{AB}, \alpha_{AC} > 0, \tag{2.95}$$

and reaches P_0, which is realized by the configuration D_1; whereas the latter passes C_2, then moves in the region γ_2, satisfying

$$\alpha_{AB} < 0,\ \alpha_{AC}, \alpha_{BC} > 0, \tag{2.96}$$

and reaches P_0, which is realized by the configuration $\tilde{D}_2$ with an appropriately chosen set of values (s,t). A similar situation is also observed for the pair R_2 and $\tilde{R}_1$.

Thus we have answered questions (2.18) and (2.19) in a positive way by following up on the movement of LN diagrams.

By the reasoning given so far, we have demonstrated how manipulation of LN diagrams is helpful in understanding LN geometry. After such a study the reader will be able to better appreciate the precise figure of $L^\times(T_1)$ ([HK2, Section 1]), which is drawn with the help of a computer. Actually the reader will notice Whitney's umbrella near Δ in the concrete visualization of $[L^\times(T_1)]$. Furthermore the appearance of Whitney's umbrella in LN surfaces is, interestingly enough, a rather universal phenomenon, as our computer-assisted study ([HK2]) indicates. Still more important is the fact that Whitney's umbrella plays an important role in understanding the mechanism how an acnode appears in $[L^\times(T_2)]$, as is shown in [HK3, Section 4].

§ 3. Sato's postulates

In this section we first recall Sato's postulates on the S-matrix, and then we add some comments to the original statement of Sato, which will be helpful to polish them up. In this section we do not assume $\nu = 2$. (What we have in mind is basically the situation in $\nu = 4$.)

Sato's postulates ([S]):

Postulate I. (i) S.S.(S), the singularity spectrum of the S-matrix S, is contained

$$\bigcup_G \mathscr{L}^+(G), \tag{3.1}$$

where G ranges over all possible Feynman graphs.

(ii) At each point (p_0, u_0) of the singularity spectrum of S, excepting those points to be specified by (3.5) below, S satisfies a holonomic system which has

(3.2) $$\bigcup_G \mathscr{L}^{\mathbb{C}}(G)$$

as its characteristic variety, where

(3.3) $\mathscr{L}^{\mathbb{C}}(G)$ denotes the complexification of $\mathscr{L}(G)$,

and furthermore

(3.4) This holonomic system is of the same nature as the one satisfied by the corresponding Feynman integral. (The last part of the statement is not satisfactory and need further clarification —— this is a future problem.)

(3.5) In the above Postulate I(ii) one has to exclude those points where an infinite number of $\mathscr{L}^{\mathbb{C}}(G)$ clusters.

Postulate II. The S-matrix S satisfies the generalized unitarity relation in the sense of Nishijima ([N]).

The above postulates, particularly Postulate I is a challenging and substantially novel proposal to shed a new light on the analytic S-matrix theory from the viewpoint of microlocal analysis, that is, a proposal of

Micro-analytic S-matrix Theory.

Actually, in response to Sato's proposal, [KS] validates that the S-matrix S satisfies a simple holonomic system at an invertible point ([KS, Definition 6]). But, at the same time, it is evident that at m-particle ($m \geq 3$) threshold points ($= m$-PT), for example at $L^{\oplus}$ (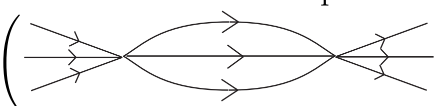) (3PT ($=m$-PT with $m = 3$)), the holonomicity fails because of the arbitrarily higher powers of the logarithmic function contained in the Feynman integrals having their singularity at m-PT. Thus it is necessary for us to polish up the above postulates, including the clarification of the proviso (3.5). The comments we give below are the starting point of our study in this direction.

[I] Comments on Postulate I.(i).

(I.a) If we could confirm the Borel summability of the perturbation series expansion of S in the coupling constants (in the energy-momentum space), then Postulate I.(i) would become a "theorem" that could be established through microlocal analysis of Feynman integrals which appear in the coefficients of the perturbation series. In conjunction with the Borel summability, we note that even if the Borel transform of the formal series

contains singularities on the real (positive) axis, there is a big hope to be able to find the path of integration defining an appropriate resummation so that the resulting sum may satisfy the unitarity relation. Probably this is one of the important lessons we have learned from the resurgent function theory.
(I.b) As we touched upon in Remark 1.5, the importance of the cotangent vectors in describing the singularity structure of the S-matrix was first recognized by H. P. Stapp and his collaborators ([CS], [IS]), independently of the advent of the theory of microfunctions. The starting point of their study is the macroscopic causality conditions on the S-matrix.

[II] Comments on (3.3) and (3.5).
(II.a) As we have discussed in [HK3, Section 4], the meaning of $\mathscr{L}^{\mathbb{C}}(G)$ should be understood as a local complexification at the present stage. If we consider the algebraic complexification of LN varieties, the geometric situation becomes much more complicated. Hence we currently restrict our consideration to the local complexification of LN varieties, although we wish the global complexification should be studied in some future. An important comment to be added here is that, as the reasoning in [HK3] shows, noticing Whitney's umbrella in LN surfaces is an important step in our consideration of problems related to their complexification.
(II.b) Even if we restrict our consideration to the local complexification of LN varieties and further ignore their multiplicity issues, the concrete content of the proviso (3.5) is not clear. Hence, as the first trial, we have studied in [HKS] assuming $\nu = 2$, the concrete structure near 3PT of locally complexified LN surface $L^{\mathbb{C}}(h_q)$ for a Feynman graph h_q in some particular class of graphs called hooked 3-lines, which is designed to study the perturbation series expansion of the 3 to 3 S-matrix element. And, we have found that, outside a tiny exceptional set N given by (3.6) below, in a small complex neighborhood of P_0 in (3PT)$\backslash N$, finitely many $L^{\mathbb{C}}(h_q)$ are relevant; otherwise stated, we have proposed N as the concrete exceptional set in the particular situation considered in [HKS].

$$N = N_+ \cup N_- \subset \{(p_1, p_2, \cdots, p_6) \in \mathbb{R}^{12}\}, \tag{3.6}$$

where

$$N_+ = \bigcup_{k^2=m^2} \{(p_1, p_2, p_3) \in \mathbb{R}^6;\ p_{\sigma(1)} = k \text{ and } p_{\sigma(2)} + p_{\sigma(3)} = 2k \text{ for a permutation } \sigma \text{ of } \{1, 2, 3\}\}, \tag{3.7}$$

$$N_- = \bigcup_{k^2=m^2} \{(p_4, p_5, p_6) \in \mathbb{R}^6;\ p_{\tau(4)} = k \text{ and } p_{\tau(5)} + p_{\tau(6)} = 2k \text{ for a permutation } \tau \text{ of } \{4, 5, 6\}\}. \tag{3.8}$$

We also need

(3.9)
$$N_0 = N_+ \cap N_- \subset \mathbb{R}^{10} = \{(p_1, p_2, \cdots, p_6) \in \mathbb{R}^{12}; p_1 + p_2 + p_3 = p_4 + p_5 + p_6\}$$

in our discussion. Actually in our proof of the finiteness of relevant LN surfaces, a crucial step was to show

(3.10)
$$L^{\oplus}(T_n) \subset N_0 \text{ for } n \geq 4,$$

where T_n is a truss-bridge diagram with n trusses given below:

(3.11)

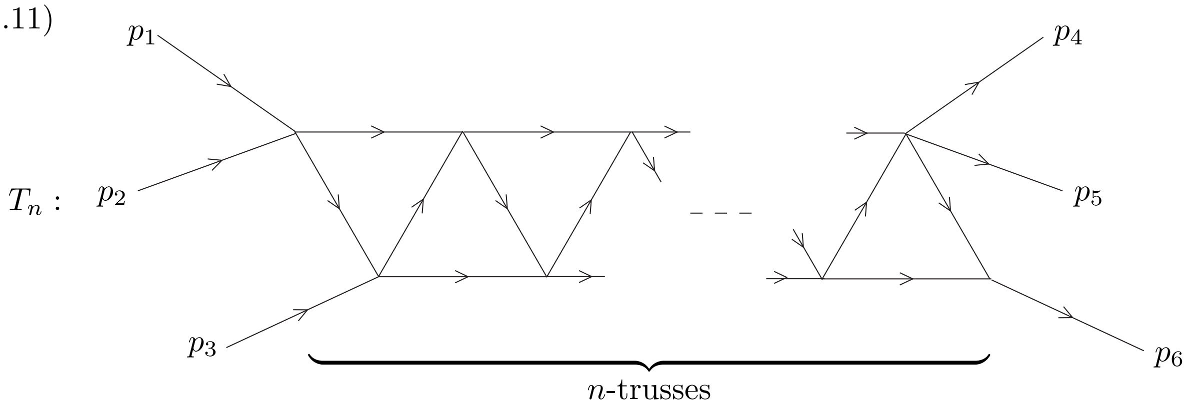

Remark 3.1. It is clear that T_1 is the triangle Feynman graph (with equal mass) given in (1.11).

Remark 3.2. To illustrate the role of $N_\pm$ we note the following:

(3.12) $L^{\oplus}$ (

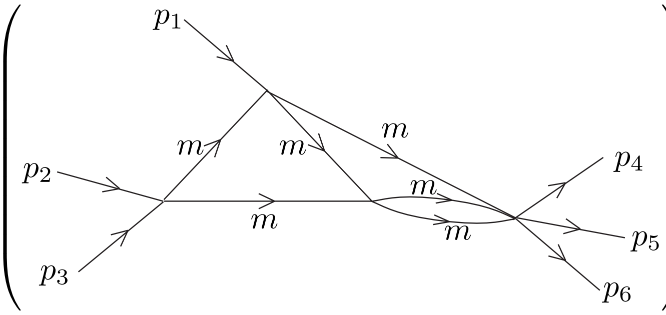

) $\subset N_+$,

(3.13) $L^{\oplus}$ (

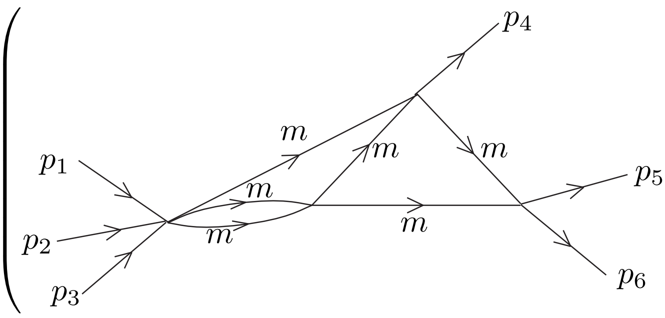

) $\subset N_-$.

Remark 3.3. One noteworthy feature of the set N is that at least one external line, i.e., $p_{\sigma(1)}$ or $p_{\tau(4)}$, is automatically confined to the mass-shell manifold.

[III] Comments on (3.4)**.**

(III.a) (3.4) is a faithful copy of the original statement in [S], and it is encouraging to find that Sato was highly interested in the analysis of Feynman integrals in the study of micro-analytic S-matrix theory. We believe what Sato wanted to propose here is to study the hierarchical principle for the S-matrix (cf. [E] for example) in the framework of microlocal analysis. Here the "hierarchical principle" means, in its most primitive form, to relate the Feynman integral F_G with $F_{\tau_1(G)}$ for the simple contraction $\tau_1(G)$ of a Feynman graph G near $[L^{\oplus}(G)] \cap L^{\oplus}(\tau_1(G))$, where $\tau_1(G)$ is, by definition, a Feynman graph obtained from G by deleting exactly one internal line L_l (and re-labelling in $\tau_1(G)$ the remaining internal line if necessary) and identifying vertices W_l^+ and W_l^- to define a new vertex $\tilde{V}$ in $\tau_1(G)$, as is illustrated by the following example:

(3.14) The simple contraction $\tau_1(T_1)$ of T_1 at the third internal line L_3 is as follows:

$\tau_1(T_1)$:
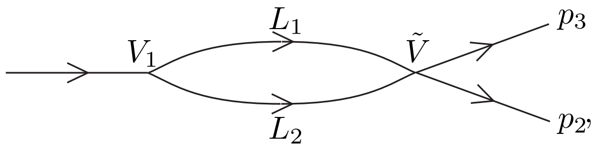

with T_1 labelled as below:

T_1 :
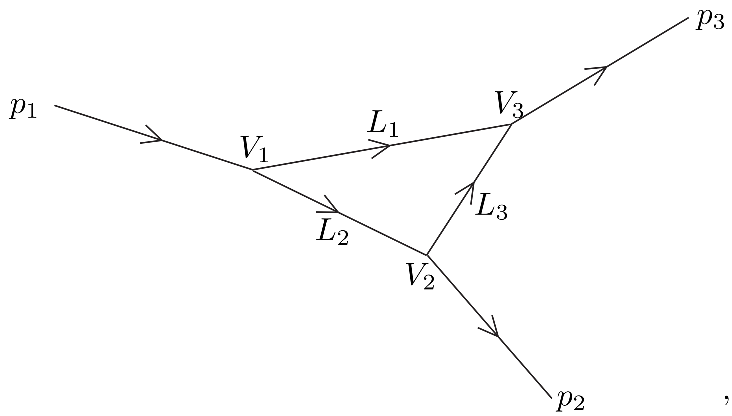

,

where $W_3^+ = V_3$ and $W_3^- = V_2$.

We also note that $[L^{\oplus}(G)] \cap L^{\oplus}(\tau_1(G))$ with $G = T_1$ corresponds to C_1 in (2.12) in this case.

We want to further add the following two comments, which we hope to give us some clues for our better understanding of the hierarchical principle in micro-analytic S-matrix theory.

(III.b) Let us consider the following simple contraction $\tau_1(T_2)$ of T_2:

(3.15) T_2 :

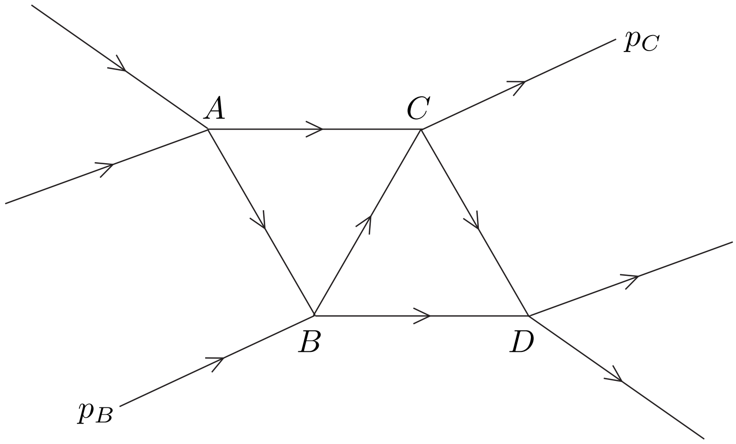

,

(3.16) $\tau_1(T_2)$:

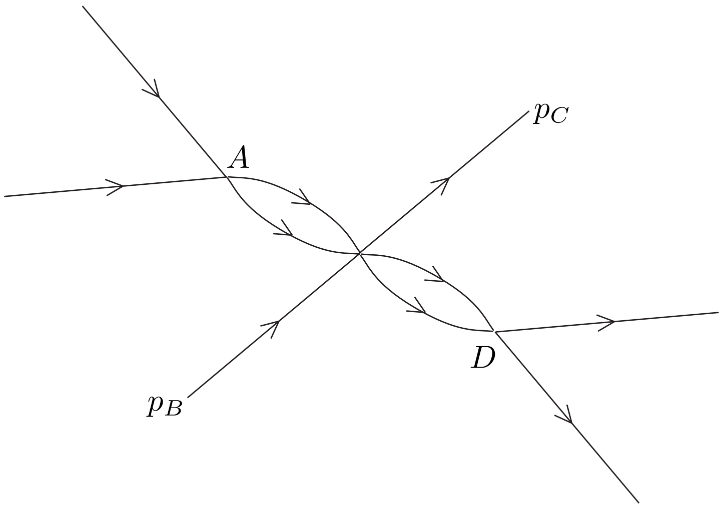

.

In this situation we find that

(3.17) $\mathrm{codim} L^{\oplus}(\tau_1(T_2))$ is 2,

and that

(3.18) a pinch point of $[L^{\times}(T_2)]$ is contained in $[L^{\oplus}(T_2)] \cap L^{\oplus}(\tau_1(T_2))$.

We refer the reader to [HK3, Section 3] for the definition of a "pinch point" used here. The pinch point referred to in (3.18) is $(P3)$ in the notation of [HK3, Section 3.2]. We note that the appearance of a pinch point in a simple contraction is observed rather universally where the LN surface associated with the simple contraction is of codimension 2. For example the pinch point (II.c) in $[L^{\oplus}(\tilde{T}_3)]$ (cf. [HK3, Section 5.2]) is contained in

(3.19) $$[L^{\oplus}(\tilde{T}_3)] \cap L^{\oplus}(\tau_1(\tilde{T}_3)),$$

where

(3.20) $\tau_1(\tilde{T}_3)$:

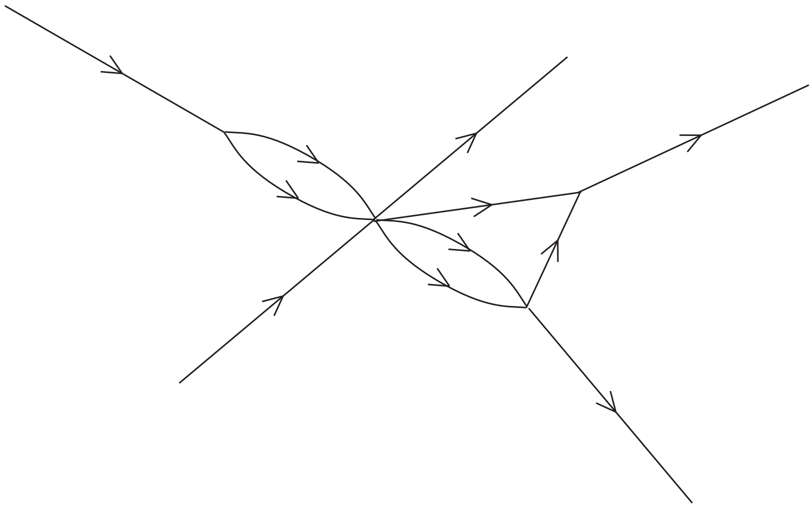

and

(3.21) $\mathrm{codim} L^{\oplus}(\tau_1(\tilde{T}_3))$ is 2.

A similar situation is observed for pinch point (III.a); this time $\tau_1(\tilde{T}_3)$ is given by

(3.22)

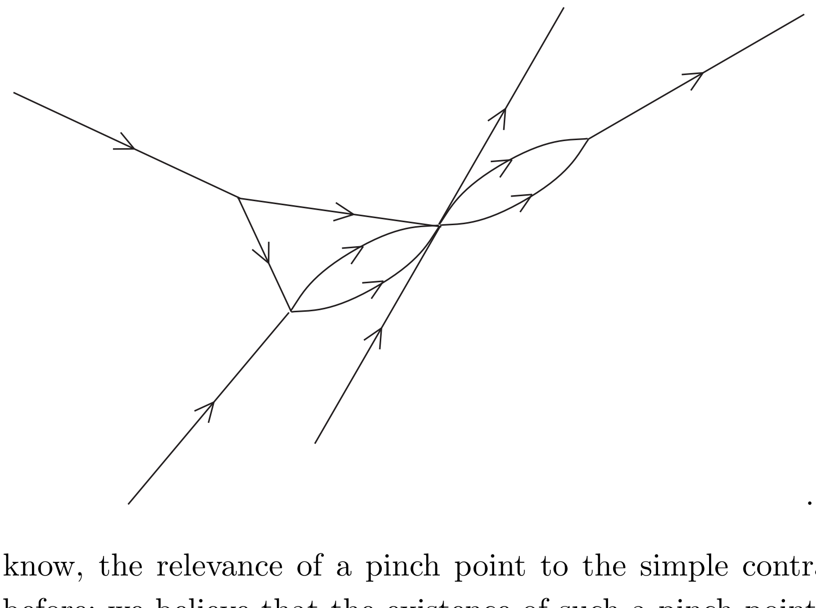

.

As far as we know, the relevance of a pinch point to the simple contraction has not been realized before; we believe that the existence of such a pinch point should be the main reason for the difficulty in analyzing the hierarchical relation when the leading positive-α LN "surface" associated with the simple contraction is of codimension 2. More detailed discussions will be given in our forthcoming paper ([HK4]).
(III.c) The geometric situation that is presented by the pair of T_1 and its simple contraction D_1 given in (2.29) seems to be very intriguing. In this case we find that

(3.23) $\mathrm{codim} L^{\times}(D_1)$ is 2, and that

(3.24) $\mathscr{L}^\times(D_1) \setminus (\mathscr{L}^\times(D_1) \cap [\mathscr{L}^\times(T_1)])$ is not contained in S.S.I_{T_1}, i.e., the singularity spectrum of I_{T_1}.

In particular (3.24) implies that the singularities of I_{T_1} along $\{\varphi_1 = 0\}$ and those along $\{\varphi_2 = 0\}$ in the notation of (2.94) are microlocally disjoint near $\pi^{-1}(P_0)$ for P_0 in Δ, where π stands for the projection from $S^*\mathbb{R}^3$ to $\mathbb{R}^3$. Here we note that Δ is the simplest example of a cusp in Whitney's umbrella. (Cf. [HK3, Section 3])

§ 4. Applications of complemented graphs

In studying LN geometry associated with a Feynman graph G which contains a non-external vertex, we have encountered several unexpected but interesting phenomena even in $L^+(G)$; one important example is the relation (3.10) (cf. Remark 3.3), and another important example is the existence of higher codimensional component in $L^\oplus(T_3)$ for the truss bridge diagram T_3:

(4.1) T_3 :

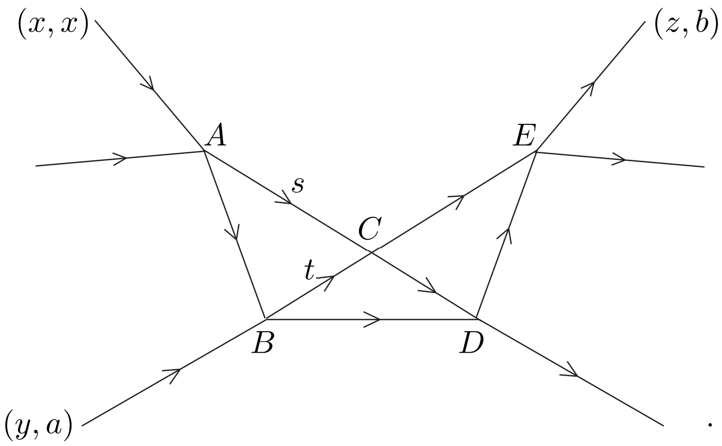

.

Here, and in the rest of this section, we assume $\nu = 2$, and use the symbols as in Section 2. For example, the symbol s put on the internal line AC means the vector associated with the internal line is (s, s^{-1}) $(s > 0)$. The symbols (y, a) and (z, b) indicate that, as is explained in [HK2], we use the slices with parameters (a, b) of $[L^\times(T_3)]$ to visualize it. A non-external vertex is, by definition, a vertex upon which no external line is incident; the vertex C in T_3 is one typical example. In order to understand pathological situations relevant to the existence of non-external vertices, we have introduced the notion of a complemented graph $\tilde{G}$ in [HK3]. Here a complemented graph $\tilde{G}$ is obtained by adding an external vector to each non-external vertex of a graph G containing non-external vertices. For example, the complemented graph $\tilde{T}_3$ of T_3 is given as follows:

(4.2)

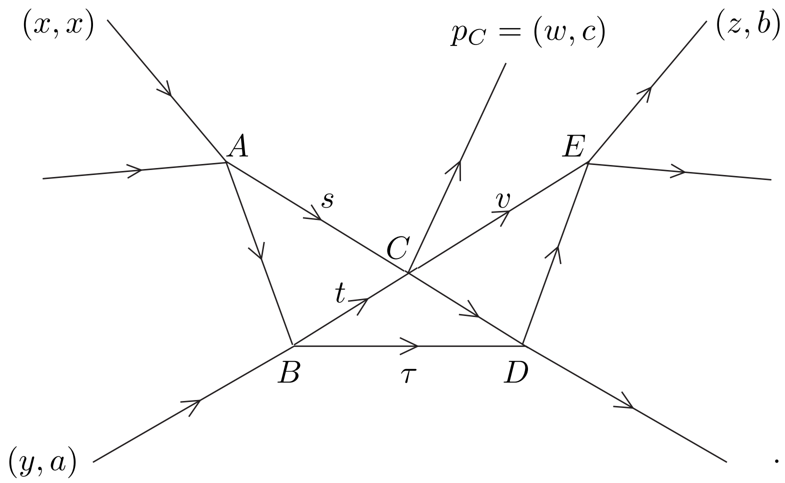

We refer the reader to [HK3, Section 5] concerning the detailed information about the relation of $L^\times(T_3)$ and $L^\times(\tilde{T}_3)$; the most interesting result among them is the following:

(4.3) The higher codimensional component of $L^\oplus(T_3)$ is given by the restriction to $\{p_C = 0\}$ of a particular pinch points set called (I.a) in [HK3].

Now besides the geometric problems discussed in [HK3], we note that the so-called $u = 0$ points ([KS]) are relevant to Feynman graphs with non-external vertices. Let us recall that a point p is, by definition, a $u = 0$ point if $(p, u) = (p, 0)$ is a non-trivial (i.e., some $\alpha_l \neq 0$) solution of LN equations associated with a Feynman graph G. A typical example of such a graph G is given by the following:

(4.4) G :

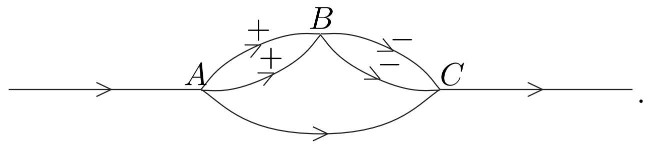

Here the symbol + (resp., −) attached to an internal line indicates that the LN constant associated with the internal line is strictly positive (resp., negative). We note that the vertex B of G in (4.4) is non-external. We also note that we encounter $u = 0$ points in a natural manner when we deal with the unitarity relation for the S-matrix.

We now try to shed a new light upon the $u = 0$ point problem by using complemented graphs. To be more specific, we first show that I_{T_3} is locally expressed as $I_{\tilde{T}_3}|_{\{p_C=0\}}$ under some geometric assumptions.

Let us consider a generic point $\tilde{p} = (p, p_C)$ of $L^\times(\tilde{T}_3)$, where $L^\times(\tilde{T}_3)$ is locally given by $\{\tilde{\varphi}(\tilde{p}) = 0\}$. Then by using the theory of holonomic (= maximally over-determined) systems ([SKK]), we find that, near the point in question, say $\tilde{p}_0 = (p_0, p_{C,0})$, the phase space integral $I_{\tilde{T}_3}(\tilde{p})$ has the form

$$\tilde{a}(\tilde{p})\delta(\tilde{\varphi}(p)), \tag{4.5}$$

where $\tilde{a}(\tilde{p})$ is a real-valued real analytic function defined near $\tilde{p}_0$. Here we note that we have used the fact that $\tilde{T}_3$ is free from non-external vertices in confirming that $I_{\tilde{T}_3}(\tilde{p})$ satisfies a simple holonomic system of order 1/2. We also note that $I_{\tilde{T}_3}(\tilde{p})$ is a real-valued hyperfunction. As $\tilde{p}_0$ is in $L^\times(\tilde{T}_3)$, we find

$$\alpha_{AB} \neq 0,\ \alpha_{DE} \neq 0. \tag{4.6}$$

Then it follows from (4.6) that

$$\mathrm{grad}_p \tilde{\varphi}(p, 0)|_{p=p_0} \neq 0. \tag{4.7}$$

Therefore the restriction of $I_{\tilde{T}_3}(\tilde{p})$ to $\{p_C = 0\}$ is well-defined and we obtain

$$I_{T_3}(p) = \tilde{a}(p, 0)\delta(\tilde{\varphi}(p, 0)) \tag{4.8}$$

near $p = p_0$.

The reasoning given above shows how effectively we can use a complemented graph $\tilde{G}$ of G in analyzing the phase space integral I_G when G contains non-external vertices. But one might raise the following question:

(4.9) By the successive contraction of internal lines AB and DE in T_3 we find the graph G in (4.4). Doesn't this cause a problem in restricting $I_{\tilde{T}_3}(\tilde{p})$ to $\{p_C = 0\}$?

It is true that the totality of $u = 0$ points for the graph G covers an open set. Actually the set of $u = 0$ points for the graph G in (4.4) is the cusp for the triangle graph $\hat{T}_1$ with non-equal masses:

(4.10) $\hat{T}_1$:

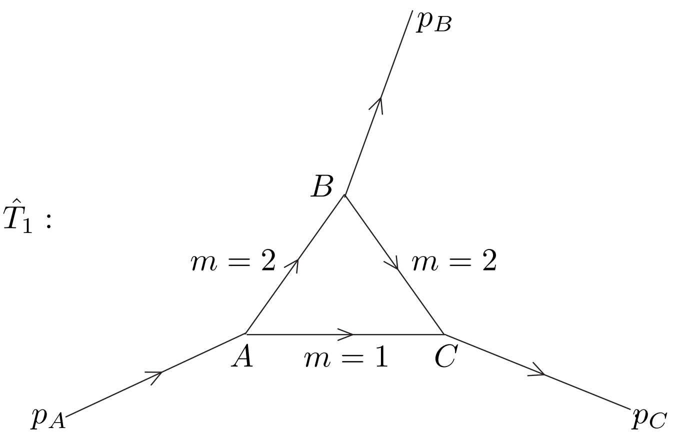

The cusp (together with its endpoint, i.e., a pinch point) for $\hat{T}_1$ is given by

$$x = y = z \geq 3, \tag{4.11}$$

if we use a coordinate system (x, y, z) such that

$$p_A = (x, x),\ p_C = (y, z). \tag{4.12}$$

On the other hand a $u=0$ point for G in (4.4) is given by the following configuration:

(4.13) 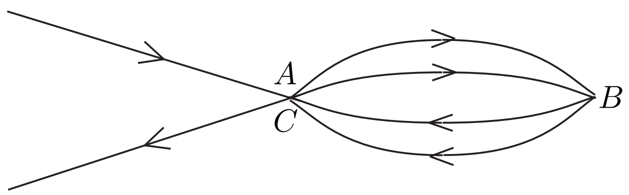 with $u_A \neq u_B$;

hence it is contained in the cusp of $\hat{T}_1$.

Thus question (4.9) seems to be reasonable. However, concerning $I_{\tilde{T}_3}$ we know

(4.14) singular points of $I_{\tilde{T}_3}$ are contained in $[L^\times(\tilde{T}_3)]$.

This means, in particular, even if

$$\alpha_{AB} = 0 \quad \text{in} \quad [L^\times(\tilde{T}_3)] \tag{4.15}$$

we still find τ in (4.2) is given by

$$(s + a - t^{-1})^{-1} \quad \text{with} \quad s = t, \tag{4.16}$$

i.e.,

$$t/[(t+a)t - 1]. \tag{4.17}$$

As we are considering the restriction of $I_{\tilde{T}_3}(\tilde{p})$ to $\{p_C = 0\}$ on a neighborhood of $L^\times(\tilde{T}_3)$, where τ is

$$t/[(s+a)t - 1] \quad \text{with} \quad s \neq t \tag{4.18}$$

the restriction procedure is legitimate. At the same time, if we consider the following integral $\hat{F}(\tilde{p})$ given by (4.19), the situation is completely different.

$$\hat{F}(\tilde{p}) = \frac{1}{(2\pi)^6} \int \cdots \int \Big(\prod_{j=1}^{5} \delta^2 \Big(\sum_r [j:r] p_r + \sum_l [j:l] k_r \Big) \Big) \delta^+(k_4^2 - 1) \times \Big(\prod_{l=1}^{3} \frac{1}{(k_l^2 - 1 + i0)} \prod_{l=5}^{7} \frac{1}{(k_l^2 - 1 - i0)} \Big) \prod_{l=1}^{7} d^2 k_l, \tag{4.19}$$

where the suffix l corresponds to the labelling the internal lines of $\tilde{T}_3$ shown below:

(4.20)

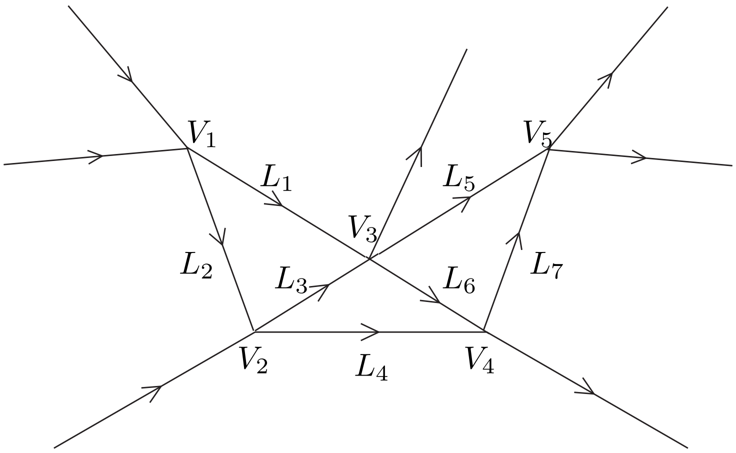

We note that by the decomposition of $\delta(k_l^2-1)$ into $-\frac{1}{2\pi i}\left(\frac{1}{k_l^2-1+i0}-\frac{1}{k_l^2-1-i0}\right)$ in the integrand of $I_{\tilde{T}_3}(\tilde{p})$ we find $\hat{F}$ among several terms appearing after the decomposition (except for the factor $\prod_{l\neq 4} Y(k_{l,0})$).

In describing the singularities of $\hat{F}$, we have to take into account the LN surface associated with the contracted graph $\tilde{G}$ given in (4.21) below, as the "propagator" $(k_l^2-1\pm i0)^{-1}$ does not vanish even when $k_l^2 \neq 1$, making a clear contrast to $\delta(k_l^2-1)$.

(4.21) $\tilde{G}$:

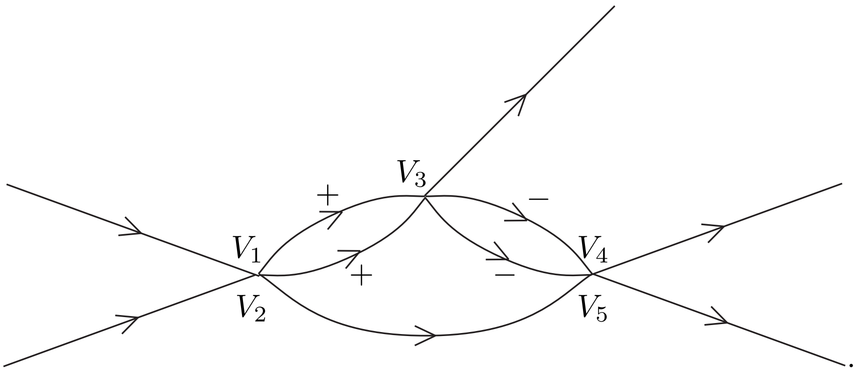

Furthermore it follows from the hierarchical principle for Feynman integrals ([SW], [S, p.23]) $\hat{F}$ contains a factor $F_{\tilde{G}}$ (with $\pm i0$ in the "propagator" being chosen according as the $\pm$ label in $\tilde{G}$ and with $\delta^+(k_4^2-1)$ being assigned to L_4). Thus the $u=0$ points for G in (4.4) may cause the divergence of the integral when p_C approaches to 0, although it might be cancelled by the background analytic functions in $\hat{F}$. We also note that the (logarithmic) divergence observed above is due to our assumption $\nu=2$. Actually we can confirm by the theory of holonomic systems that the singularity of $F_{\tilde{G}}$ has the form $\varphi^3 \log \varphi$ with $\varphi(p,p_C)|_{p_C=0}$ being 0, if we consider the same problem assuming $\nu=4$. This means that we should be careful about the singularity of $\hat{F}$ in manipulating the unitarity relation for the S-matrix when $\nu=2$; we have not yet seriously thought over this point, but we believe it should be worth being recorded.

§ 5. Future problems and concluding remarks

By studying some basic examples in micro-analytic S-matrix theory we have so far shown how the trials toward the better understanding of Sato's postulates lead us to find novel and intriguing problems in microlocal analysis. In this section we present some concrete problems which we hope to be useful for developing the research in this direction further.

[**A**] It should be an interesting problem to try to find the concrete form of solutions of a simple holonomic system when the projection of its characteristic variety to the base manifold contains Whitney's umbrella. Actually we have not yet known even the concrete form of I_{T_1} (other than the integral representation, i.e., its definition) near the pinch point of $L^{\oplus}(T_1)$.

[**B**] It is an interesting problem to find the concrete form of $I_{\tilde{T}_3}$ near the pinch point (I.a) (in the notation of [HK3]) and then apply the result to find the explicit form of I_{T_3} near the higher codimensional component of $L^{\oplus}(T_3)$. We believe that its holonomic structure is different from that of I_h, where h stands for the hinged graph

(5.1)

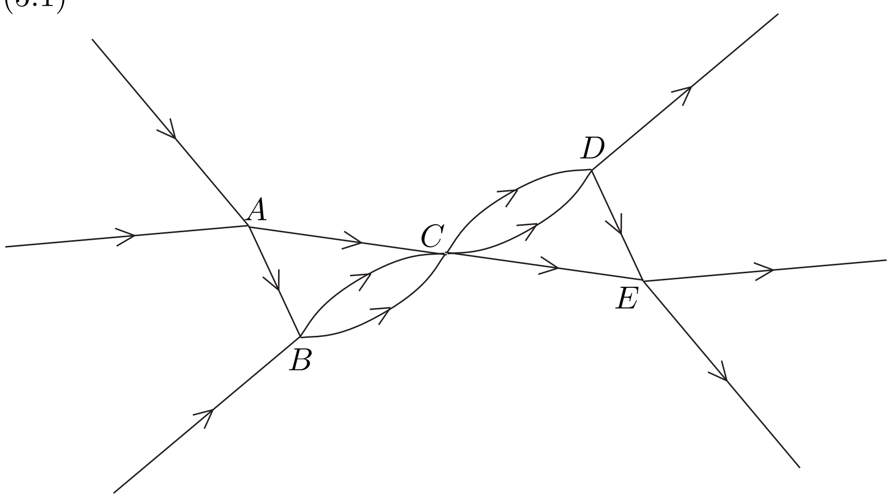

with $\alpha_{AB}, \alpha_{DE} \neq 0$.

Here we note that $L^{\oplus}(h)$ geometrically coincides with the higher codimensional component of $L^{\oplus}(T_3)$.

[**C**] In parallel with trying to answer these questions, we should try to use a computer to write down the explicit form of the simple holonomic system that $I_{\tilde{T}_n}$ satisfies.

[**D**] In the analysis with the help of a computer, the study of the holonomic structure of Feynman integrals is more difficult than that of phase space integrals. At the same time, the analytic renormalization of Speer ([Sp]) is an excellent procedure which nicely fits in with microlocal analysis fortified with a computer. In this direction of the research, the study of the holonomic structure of F_{T_n} near $3PT$ is the first trial to be done in conjunction with Postulate I (ii); clarifying the holonomic structure of F_{T_n} will help to clarify what kind of holonomic systems Sato had in mind there. Here we note that, despite the inclusion relation (3.10), $L^+(T_n)$ is, unlike $L^\oplus(T_n)$, a rather large set worth studying. For example

$$L^\oplus(h) \subset L^+(T_4) \tag{5.2}$$

holds for h given by (5.1), and furthermore, we find

$$(3PT) \subset [L^\oplus(h)]. \tag{5.3}$$

[E] Although the study of the (holonomic) structure of the S-matrix near the exceptional set N is a formidable task because of the failure of the finiteness of the number of the relevant LN surfaces there, the study of individual Feynman integrals near N is, in principle, within reach of us, microlocal analysts. Actually in view of the exceptional geometric features of LN surfaces near N (versus "outside N") ([HKS, Appendix B], [HK2, Section 3.3]) we believe the study of holonomic structure of F_G near N should be a mathematically important and challenging problem.

In this paper we have put our emphasis on the study of phase space integrals rather than Feynman integrals, particularly in the computation of integrals associated with complemented graphs, as the phase space integrals are often more suited for the concrete computation. However, particularly in studying the hierarchical principle for the S-matrix, Feynman integrals are more suited for our purpose. Actually in the analytic S-matrix theory we are forced to analyze "bubble diagram functions" ([KS]) in manipulating the unitarity relation; if we regard the S-matrix as the Borel sum of a formal series with Feynman integrals as its coefficients, a bubble diagram function is, in a rough description, a phase space integral whose vertex δ-function (i.e., the δ-function $\delta^\nu\big(\sum_r[j;r]p_r + \sum_l[j;l]k_l\big)$ at the vertex V_j) is replaced by a Feynman integral or its complex conjugate. Thus the integral $\hat{F}(\tilde{p})$ given in (4.19) is one of the simplest examples of bubble diagram functions. As we touched upon there, such integrals are, in principle, coupled with the $u = 0$ problem. We believe that the employment of complemented graphs should be useful in analyzing integrals suffering from the $u = 0$ trouble, and that it nicely fits in with Sato's intention in emphasizing the generalized unitarity, rather than the unitarity, in stating Postulate II.

References

[CS] C. Chandler and H. P. Stapp: Macroscopic causality conditions and properties of scattering amplitudes, J. Math. Phys., **10**(1969), 826–859.

[E] R. J. Eden, P. V. Landshoff, D. I. Olive and J. C. Polkinghorne: The Analytic S-Matrix, Cambridge Univ. Press, 1966.

[HK1] N. Honda and T. Kawai: A computer-assisted study of the Landau-Nakanishi geometry, RIMS Kôkyûroku, **1861**(2013), 100–110.

[HK2] ______: Visualization of the Landau-Nakanishi surfaces for truss-bridge graphs, RIMS Preprint 1809, 2014; available at `http://www.kurims.kyoto-u.ac.jp/preprint/index.html`.

[HK3] ______: A study of pinch points and cusps in the Landau-Nakanishi geometry, RIMS Kôkyûroku Bessatsu, **B57**(2016), 195–234.

[HK4] ______: On the relevance of a pinch point to the hierarchical problems in microanalytic S-matrix theory. (In preparation)

[HKS] N. Honda, T. Kawai and H. P. Stapp: On the geometric aspect of Sato's postulates on the S-matrix, RIMS Kôkyûroku Bessatsu, **B52**(2014), 11–54.

[IS] D. Iagolnitzer and H. P. Stapp: Macroscopic causality and physical region analyticity in S-matrix theory, Comm. Math. Phys., **14**(1969), 15–55.

[K] T. Kawai: Sato-Komatsu seminar, in "⌈Gekidou no 20seiki sûgaku⌋ o kataru", Kyôritsu, Tokyo. (In press; in Japanese)

[KS] T. Kawai and H. P. Stapp: Microlocal study of S-matrix singularity structure, Lect. Notes in Phys., **39**(1975), Springer, 38–48.

[N] K. Nishijima: Asymptotic conditions and perturbation theory, Phys. Rev., **119**(1960), 485–498.

[S] M. Sato: Recent development in hyperfunction theory and its applications to physics (Microlocal analysis of S-matrix and related quantities), Lect. Notes in Phys., **39**(1975), Springer, 13–29.

[SKK] M. Sato, T. Kawai and M. Kashiwara: Microfunctions and pseudo-differential equations, Lect. Notes in Math., **287**(1973), Springer, 265–529.

[Sp] E. R. Speer: Generalized Feynman Amplitudes, Princeton Univ. Press, 1969.

[SW] E. R. Speer and M. J. Westwater: Generic Feynman amplitudes, Ann. Inst. H. Poincaré, **14**(1971), 1–55.